Role of the Dimethylbenzimidazole Tail in the Reaction Catalyzed by Coenzyme B_{12}-Dependent Methylmalonyl-CoA Mutase[†]

Shantanu Chowdhury and Ruma Banerjee*

Department of Biochemistry, University of Nebraska, Lincoln, Nebraska 68588-0664

Received June 28, 1999; Revised Manuscript Received September 8, 1999

ABSTRACT: The recent structures of cobalamin-dependent methionine synthase and methylmalonyl-CoA mutase have revealed a striking conformational change that accompanies cofactor binding to these proteins. Alkylcobalamins have octahedral geometry in solution at physiological pH, and the lower axial coordination position is occupied by the nucleotide, dimethylbenzimidazole ribose phosphate, that is attached to one of the pyrrole rings of the corrin macrocycle via an aminopropanol moiety. In contrast, in the active sites of these two B_{12}-dependent enzymes, the nucleotide tail is held in an extended conformation in which the base is far removed from the cobalt in cobalamin. Instead, a histidine residue donated by the protein replaces the displaced intramolecular base. This unexpected mode of cofactor binding in a subgroup of B_{12}-dependent enzymes has raised the question of what role the nucleotide loop plays in cofactor binding and catalysis. To address this question, we have synthesized and characterized two truncated cofactor analogues: adenosylcobinamide and adenosylcobinamide phosphate methyl ester, lacking the nucleotide and nucleoside moieties, respectively. Our studies reveal that the nucleotide tail has a modest effect on the strength of cofactor binding, contributing ~1 kcal/mol to binding. In contrast, the nucleotide has a profound influence on organizing the active site for catalysis, as evidenced by the retention of the base-off conformation in the truncated cofactor analogues bound to the mutase and by their inability to support catalysis. Characterization of the kinetics of adenosylcobalamin (AdoCbl) binding by stopped-flow fluorescence spectroscopy reveals a pH-sensitive step that titrates to a pK_a of 7.32 ± 0.19 that is significantly different from the pK_a of 3.7 for dimethylbenzimidazole in free AdoCbl. In contrast, the truncated cofactors associate very rapidly with the enzyme at rates that are too fast to measure. Based on these observations, we propose a model in which the base-on to base-off conformational change is slow and is assisted by the enzyme, and is followed by a rapid docking of the cofactor in the active site.

Corrinoids are cobalt-containing organometallic cofactors found in the microbial and animal kingdoms. They are unique among the family of tetrapyrrolic derived macrocyclic cofactors in having a nucleotide tail appended from one of the pyrrole rings (ring D). A number of unusual bases have been identified in nature as components of the nucleotide tail, and, depending on their structure, either do or do not provide the lower axial ligand to the cobalt in solution. In non-cobalamin corrinoids, the bases that have been described in this position include 5-hydroxybenzimidazole, 5-methoxybenzimidazole, naphthimidazole, benzimidazole, paracresol, 5-methylbenzimidazole, and 2′-methyladenine. In cobalamin, the cofactor form found in mammals, the intramolecular base is dimethylbenzimidazole, and provides the lower axial nitrogen ligand to the cobalt in solution at physiological pH (Figure 1). The diversity in the structures of the nucleotide bases raises questions about their role(s) in corrinoid-dependent reactions.

Coenzyme B_{12} (or AdoCbl)[1]-dependent enzymes catalyze a variety of 1,2 rearrangement reactions in nature. Spectroscopic and structural studies reveal that there are at least two very different conformations in which AdoCbl is bound to the active site of proteins. Enzymes containing the signature cobalamin binding sequence DX**H**XXG (*1*) bind AdoCbl in the base-off conformation in which the dimethylbenzimidazole moiety is replaced as a lower ligand by a histidine residue provided by the protein. Enzymes that belong to this family include methylmalonyl-CoA mutase (*2, 3*), methylene glutarate mutase, and glutamate mutase (*4*). In addition, this motif is found in some methylcobalamin-dependent enzymes including methionine synthase (*5*) and the methanogenic methyltransferase, Mtr (*6*). In contrast, a second subgroup of isomerases binds AdoCbl in the base-on conformation, retaining the dimethylbenzimidazole ligation in the active site (*7, 8*).

Methylmalonyl-CoA mutase catalyzes the reversible isomerization of methylmalonyl-CoA to succinyl-CoA, and is the only member of the isomerase family found in both microbes and animals (*9, 10*). An extensive literature on model studies supports the potential importance of the bulky dimethylbenzimidazole ligand in rearrangement reactions (*11*−*19*). How-

[†] This work was supported by a grant from the National Institutes of Health (DK45776).

* Corresponding author. Telephone: (402)-472-2941. FAX: (402)-472-7842. Email: rbanerjee1@unl.edu.

[1] Abbreviations: AdoCbl, 5′-deoxyadenosylcobalamin; AdoCbi, 5′-deoxyadenosylcobinamide; AdoCbi-PMe, 5′-deoxyadenosylcobinamide phosphate methyl ester; OHCbi, hydroxocobinamide; OHCbl, hydroxocobalamin.

10.1021/bi9914762 CCC: $18.00
Published on Web 10/29/1999

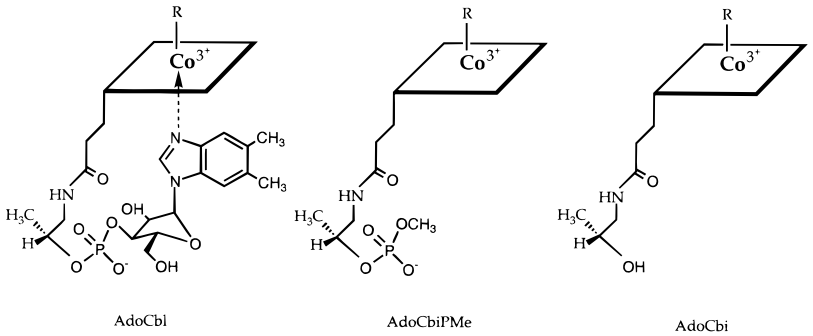

FIGURE 1: Structures of AdoCbl and its derivatives employed in this study.

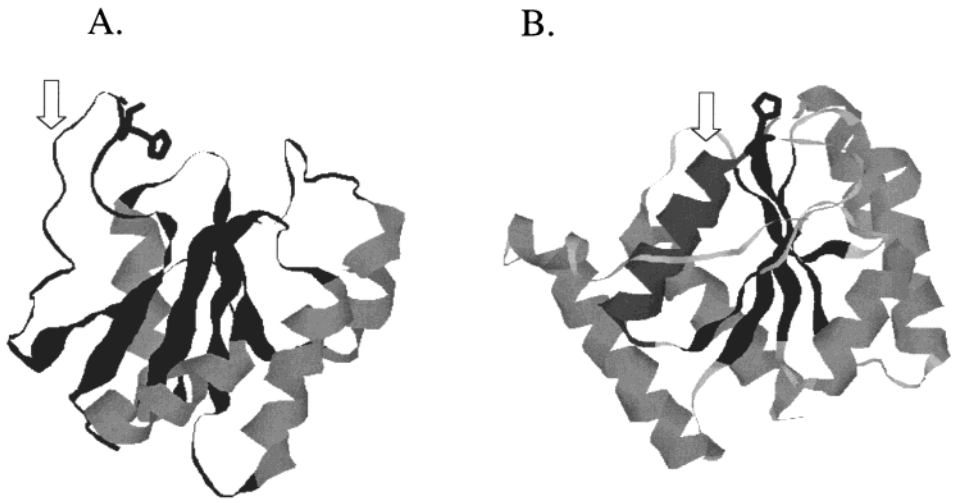

FIGURE 2: Comparison of the structures of the B_{12} binding domains of glutamate mutase (A) and holomethylmalonyl-CoA mutase (B). The figures were generated using the PDB files 1BE1 (A) and 1REQ (B). The arrows point to the region of the two proteins in which the secondary structures are different. The IIα2 helix (indicated by arrow) in methylmalonyl-CoA mutase is shown in a darker shade of gray.

ever, crystallographic (*3*, *5*) and spectroscopic (*2*, *4*) insights into the conformation of cobalamins bound to some enzymes have forced us to reevaluate the importance of the nucleotide tail. The crystal structure of methylmalonyl-CoA mutase (*3*, *20*) has revealed that cobalamin binding to the enzyme is accompanied by replacement of the dimethylbenzimidazole ligand by His610 provided by the large subunit. The nucleotide tail is bound to a C-terminal flavodoxin-like domain comprised of a five-stranded twisted parallel β-sheet structure flanked by five α-helices. Numerous electrostatic interactions between the side chain acetamides and propionamides of the corrin ring and residues in the N-terminal domain hold the corrin ring in place (*3*). In this extended conformation, the dimethylbenzimidazole is distant from the cobalt and buried in a hydrophobic pocket, and begs the following question: What role does the nucleotide tail play in this and in related enzymes?

Recently, the structure of apo-MutS, the subunit of glutamate mutase that represents the C-terminal flavodoxin-like domain in this protein, has provided insight into the structural reorganization that presumably accompanies cofactor binding (*21*). The MutS structure, lacking B_{12}, is very similar to the corresponding regions of methylmalonyl-CoA mutase and methionine synthase, indicating that this domain is largely preorganized. However, a major difference is in a segment of the protein that is folded into an α-helix and leads away from the coordinating histidine in the structures of the B_{12}-bound proteins (Figure 2). In MutS, this segment is unstructured and forms an extended mobile loop. In this study, we have evaluated the role of the tail in cofactor binding, histidine ligation, and catalysis in methylmalonyl-CoA mutase by studying two truncated cofactor analogues, AdoCbi and AdoCbi-PMe, that are missing the nucleotide or nucleoside moieties, respectively. Our results indicate the relative unimportance of the nucleotide tail to the strength of cofactor binding in contrast to its critical role in the organization of the active site for catalysis.

METHODS

Materials. Cyanocobalamin, 5′-iodo-5′-deoxyadenosine, methyl dichlorophosphate, and AdoCbl were purchased from Sigma. DEAE-cellulose, cellulose phosphate, Amberlite XAD-2, and CM-cellulose used for purifying the cofactor analogues AdoCbi and AdoCbi-PMe were also purchased from Sigma. Radioactive [^{14}C]-CH_3-malonyl-CoA (56.4 Ci/mol) was purchased from New England Nuclear. All other chemicals were reagent-grade commercial products and were used without further purification.

Enzyme Expression and Purification. The recombinant expression vector (pMEX2/pGP1-2) harboring the *P. shermanii* genes in *Escherichia coli* strain K 38 (*22*) was a gift from Peter Leadlay (Cambridge University). The enzyme was purified through the step preceding reconstitution with cofactor as described before (*23*).

Enzyme Assays. Specific activity of the mutase was determined in the radiolabeled assay at 37 °C as described previously (*24*) and was 26 units/mg of protein; 1 unit of

activity catalyzes the formation of 1 μmol of succinyl-CoA/min at 37 °C. When the ability of cofactor analogues to support catalysis was evaluated, the concentration of enzyme was increased 1000-fold (with AdoCbi) or 4000-fold (with AdoCbi-PMe) with respect to the standard assay.

Synthesis of AdoCbi and AdoCbi-PMe. AdoCbi and AdoCbi-PMe were synthesized and characterized as described previously (*25*). Both cofactor analogues were characterized by FAB-MS analysis at the Midwest Center for Mass Spectrometry at the University of Nebraska, Lincoln.

Determination of Equilibrium Binding Constants by Fluorescence Spectroscopy. Fluorescence measurements of equilibrium binding constants were made on a Perkin-Elmer LS50 luminescence spectrometer. The excitation wavelength was 282 nm (slit width, 3 μm), and emission was observed between 300 and 380 nm (slit width, 3 μm). The intrinsic tryptophan fluorescence emission of methylmalonyl-CoA mutase (monitored at 340 nm) is quenched on binding of AdoCbl. To determine the equilibrium dissociation constant, 500 μL of 0.4 μM methylmalonyl-CoA mutase in 50 mM potassium phosphate buffer, pH 7.5, was added to a quartz fluorescence cuvette, and successive aliquots (2−5 μL) of a stock 0.1 mM AdoCbl solution prepared in the same buffer were added. Following each addition, the solution was incubated at 4 °C for 30 min prior to measurement of the fluorescence emission. Free AdoCbl, even at millimolar concentrations, did not exhibit fluorescence emission between 300 and 600 nm upon excitation at 282 nm. As an additional control for nonspecific quenching, fluorescence of lysozyme was monitored on addition of millimolar concentrations of AdoCbl. No change in fluorescence emission was observed.

The fractional saturation (y) of the total AdoCbl binding sites (E_o) was obtained from the ratio $\Delta F/\Delta F_{max}$, where ΔF_{max} is the limiting value of the difference in fluorescence intensity (ΔF) approached at high concentrations of AdoCbl. The concentration of bound ligand (L_b) is related to the concentration of free ligand binding sites (E) and to the concentration of free ligand (L) by the law of mass action and the dissociation constant, K_d. Using the relations $L_b = yE_o$ and $L = L_o - yE_o$, the fractional saturation of the ligand binding sites is related to the total concentration of added ligand, L_o, as given in eq 1 (*26*):

$$1/(1 - y) = L_o/[y(1/K_d)] - E_o/K_d \quad (1)$$

A plot of $1/(1 - y)$ versus L_o was fitted to a straight line according to the above equation using the experimentally obtained value of ΔF and the known value of E_o (total concentration of methylmalonyl-CoA mutase) as constraints. The value for the dissociation constant, K_d, was obtained from the slope of the line. The K_d values for AdoCbi and AdoCbi-PMe were similarly determined. The concentration of methylmalonyl-CoA mutase used in each of these experiments was 0.25 μM.

Equilibrium Binding Constants Measured by UV−Visible Absorption Spectroscopy. Binding of AdoCbl and AdoCbi to methylmalonyl-CoA mutase was followed spectrophotometrically using a Cary-118 spectrophotometer (Olis Instruments), in which the cuvette holder was maintained at 4 °C by a thermostated water circulator. Methylmalonyl-CoA mutase (19.6 μM) in 150 μL of 50 mM potassium phosphate buffer, pH 7.5, was employed as a blank. Spectra were recorded from 800 to 306 nm after each addition of AdoCbl (3−5 μL aliquots prepared in the same buffer), following incubation at 4 °C for 30 min. The final AdoCbl concentration used in these experiments was 29 μM. The change in absorbance at 522 nm at each concentration of AdoCbl was obtained by subtracting the absorbance in a solution containing the same concentration of free AdoCbl. Since the affinity of methylmalonyl-CoA mutase for AdoCbl is high (*27*), the assumption that the total concentration of AdoCbl is equal to the free concentration of the cofactor at equilibrium does not hold. Hence, the free AdoCbl concentration was calculated assuming a single binding site (*28*), using eq 2:

$$L_b = 0.5\{E_o + L_o + K_d - [(E_o + L_o + K_d)^2 - 4E_oL_o]^{1/2}\} \quad (2)$$

where L_b is the concentration of bound ligand, E_o and L_o are the total concentrations of methylmalonyl-CoA mutase and AdoCbl, respectively, and K_d is the dissociation constant obtained from the equilibrium fluorescence experiments. The free ligand concentration (L) is given by the relation shown in eq 3:

$$L = L_o - L_b \quad (3)$$

The experimentally obtained values for $\Delta A_{522\ nm}$ were plotted versus the concentration of free AdoCbl, L, and the data were fitted using eq 4 as described in (*28*).

$$L_b = E_oL/(K_d + L) + cL \quad (4)$$

where cL is the contribution from a low-affinity nonspecific binding site with partition coefficient c, and $K_d = 0.17$ μM.

Binding of AdoCbi was followed using a similar procedure. The enzyme concentration used in this study was 32 μM, and AdoCbi was added to a final concentration of 29.7 μM. The binding isotherm was plotted using the value of ΔA_{460nm} instead of ΔA_{525} used for AdoCbl.

Stopped-Flow Fluorescence Spectroscopy. Rapid-scanning stopped-flow kinetic measurements were made using the RSM-2 software for the OLIS stopped-flow fluorescence spectrophotometer. An external water bath was used to maintain the temperature of the loading syringes at 30 °C. The concentration of AdoCbl was at least 8-fold greater than the enzyme concentration to obtain pseudo-first-order conditions. Fluorescence emission spectra were recorded between 310 and 450 nm using an emission slit width of 3.16 μm acquired at 62 scans/s or 31 scans/s depending on the time course of the decay. The excitation wavelength was 282 nm, and two consecutive slits of 0.6 μm width were used.

The concentration of enzyme used was 0.4 μM after mixing, and AdoCbl concentrations ranged from 3.4 to 15 μM after mixing. The enzyme and cofactor were prepared in potassium phosphate buffers (50 mM) with pH varying from 6 to 8.2. Fluorescence decay was observed at five different concentrations of AdoCbl at each pH. Sigmaplot (Jandel Scientific) was used to analyze the fluorescence quenching data. Best fits were obtained using eq 5:

$$F = A_i + \Delta Ae^{(-k_1t)} - k_2t \quad (5)$$

where F is the observed fluorescence at time t, ΔA is the

amplitude of exponential decay, k_1 is the rate of exponential decay, k_2 is the rate of background decay, and A_i is the offset for the exponential decay. The rate of background fluorescence decay (k_2) was recorded with 0.4 μM enzyme in the absence of ligand, and was pH-independent in the range used.

The observed k_1 value at each concentration of AdoCbl was plotted as a function of AdoCbl concentration at a given pH and was fitted to eq 6:

$$k_1 = k_{on}[\text{AdoCbl}] + k_{off} \quad (6)$$

The slope of the line represents k_{on} and was plotted as a function of pH to obtain the pK_a.

RESULTS

Fluorometric Determination of Equilibrium Binding Constants. Addition of AdoCbl to methylmalonyl-CoA mutase results in a decrease in fluorescence emission at 340 nm as shown in Figure 3A. However, the change in fluorescence is not completely saturated even at very high concentrations of AdoCbl ($>10K_d$) and is likely to result from nonspecific binding. The value of ΔF_{max}, the maximum decrease in fluorescence, used for calculating the fractional saturation, *y*, was thus chosen by inspection of the titration curves and refined so that the intercept from the plot fitted to eq 1 matched E_o (the total enzyme concentration, Figure 3A, inset). The final values of ΔF_{max} obtained from the fits were always consistent with the approximations obtained from the titration curves (see figure legends). The high affinity of AdoCbl for methylmalonyl-CoA mutase poses a limitation on the use of Scatchard analysis which assumes that the bound concentration of ligand is very small with respect to the total ligand concentration, which is the case when $K_d \gg E_o$. Under the conditions of our experiment where $E_o \approx K_d$, the data were treated according to a previously published method (*26*), as described under Methods. From this analysis, a K_d of 0.17 $\pm$ 0.012 μM is estimated, which is in excellent agreement with the value obtained by equilibrium dialysis (0.16 μM) using radiolabeled AdoCbl (Maiti, Brown, and Banerjee, unpublished data).

Similar experiments with AdoCbi (Figure 3B) and AdoCbi-PMe (Figure 3C) yielded K_d values of 0.62 $\pm$ 0.09 and 3.33 $\pm$ 0.028 μM, respectively. These results are summarized in Table 1.

UV−Visible Spectroscopic Determination of Equilibrium Binding Constants. Binding of AdoCbl to methylmalonyl-CoA mutase is accompanied by an increase in absorbance across the 300−600 nm spectral range (Figure 4). A plot of ΔA_{522} versus the concentration of free AdoCbl at equilibrium is shown (Figure 4, inset). The free ligand concentration was calculated at each point in the titration curve by using the K_d obtained from the fluorescence experiments according to eqs 2 and 3. The excellent fit for the absorbance data using the K_d value obtained from the fluorescence data indicates the correspondence between the two independent methods, and confirms that the binding isotherms monitored by fluorescence spectroscopy reflect specific binding of cofactor to the mutase.

The same procedure was followed for studying equilibrium binding of AdoCbi (Figure 5). In contrast to AdoCbl, the absorbance maximum for both AdoCbi and AdoCbi-PMe (not shown) bound to the mutase is at 460 nm rather than at 525 nm. This indicates that His610 in the large subunit is not coordinated to cobalt in the bound forms of the truncated cofactors. The fit to the binding isotherm (Figure 5, inset) again shows that the K_d values obtained for AdoCbi from the equilibrium fluorescence and UV−visible experiments are in close agreement.

Cofactor Activity of AdoCbi and AdoCbi-PMe. Activity of methylmalonyl-CoA mutase with AdoCbi could be detected only when the concentration of enzyme was increased 1000-fold with respect to the level used in the standard assay (data not shown). In the case of AdoCbi-PMe, no activity was detected even when a 4000-fold higher concentration of enzyme was employed. Since AdoCbi is synthesized from OH-Cbi derived by hydrolysis of OH-Cbl, trace contamination of AdoCbi with AdoCbl (resulting from adenosylation of residual OH-Cbl) cannot be ruled out, and, in fact, seems likely especially since AdoCbi-PMe does not support catalysis. At an ~1000-fold lower level than AdoCbi, contamination by AdoCbl would escape detection by both the mass spectroscopic and HPLC methods that were employed for analysis of purity.

Stopped-Flow Fluorescence Spectroscopy. The kinetics of tryptophan fluorescence quenching caused by binding of AdoCbl were measured under stopped-flow conditions (Figure 6). A plot of the k_{obs} for fluorescence decay as a function of ligand concentration at different pH values (Figure 7) yields values of k_{on} and k_{off} as described in eq 6. From the pH dependence of k_{on}, a pK_a of 7.32 $\pm$ 0.19 is obtained (Figure 7, inset).

DISCUSSION

Binding of AdoCbl to methylmalonyl-CoA mutase is expected to involve a significant conformational rearrangement in both the enzyme and the cofactor. The bulky and intramolecular base dimethylbenzimidazole, which is coordinated to the cobalt to give the base-on conformation in the free cofactor, must be displaced. This is replaced by coordination to His610 provided by the flavodoxin-like domain of the large subunit (*3*). In addition, a structural change is expected in the protein based on comparison of the B_{12} binding domains of apoglutamate mutase and holomethylmalonyl-CoA mutase (Figure 2). The sequence corresponding to an unstructured and extended mobile loop in apo MutS [designated α1 (*21*)] is organized into an α-helix in holomethylmalonyl-CoA mutase [helix IIα2 (*29*)]. The differences in secondary structure in this region are noteworthy since the rest of the elements in the flavodoxin-like domain are virtually superimposable in the two proteins whether or not the cofactor is present. In addition, this α-helix is immediately downstream of the loop containing two of the three residues of the catalytic triad (Asp608 and His610 in methylmalonyl-CoA mutase) that are located on the lower face of the cofactor. Hence, a comparison of the apo- and holoenzyme structures suggests that a major role of the cofactor tail may be to organize the binding pocket so as to orient His610 for coordination to cobalt in methylmalonyl-CoA mutase. To test this hypothesis, and to evaluate the contribution of the tail to binding and to catalysis, we have synthesized and characterized two truncated cofactor analogues, AdoCbi and AdoCbi-PMe.

Binding of AdoCbl is accompanied by an overall quenching in tryptophan fluorescence (Figure 3A). The large subunit

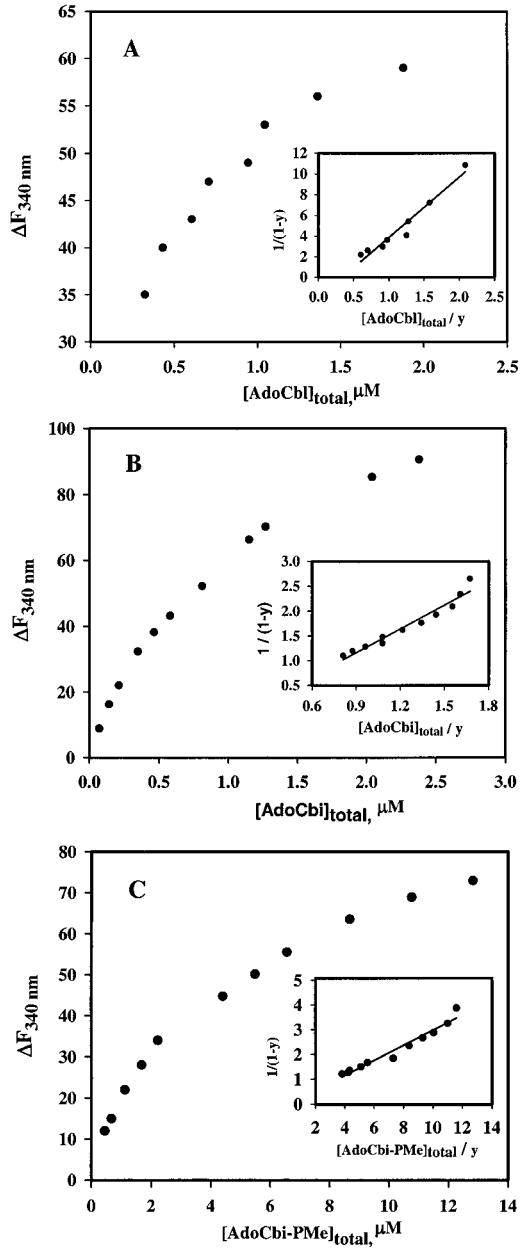

FIGURE 3: Fluorometric determination of the equilibrium binding constant for AdoCbl and its analogues. (A) Methylmalonyl-CoA mutase (0.40 μM) was titrated with AdoCbl (0.32−1.87 μM). The change in fluorescence at 340 nm is plotted as a function of total AdoCbl concentration. Inset: The fractional saturation, *y*, is plotted versus $[AdoCbl]_{total}/y$ according to eq 1. The estimated ΔF_{max} that gave the best match for E_o (0.34 ± 0.017 μM), the total concentration of binding sites, was 65 arbitrary units. The K_d determined from this analysis is 0.17 ± 0.012 μM. (B) Fluorometric determination of the equilibrium binding constant for AdoCbi. Methylmalonyl-CoA mutase (0.25 μM) was titrated with AdoCbi (0.20−2.38 μM). The change in fluorescence at 340 nm is plotted as a function of total AdoCbi concentration. Inset: Fractional saturation is plotted versus $[AdoCbi]_{total}/y$ according to eq 1. The estimated ΔF_{max} that gave the best match for E_o (0.18 ± 0.02 μM), the total concentration of binding sites, was 100 arbitrary units. The K_d determined from this analysis is 0.62 ± 0.09 μM. (C) Fluorometric determination of the equilibrium binding constant for AdoCbi-PMe. Methylmalonyl-CoA mutase (0.25 μM) was titrated with AdoCbi-PMe (0.40−12.7 μM). The change in fluorescence at 340 nm is plotted as a function of total AdoCbi-PMe concentration. Inset: The fractional saturation is plotted versus $[AdoCbi\text{-}PMe]_{total}/y$ according to eq 1. The estimated ΔF_{max} which gave the best match for E_o (0.19 ± 0.04 μM) was 85 arbitrary units. The K_d determined from this analysis is 3.33 ± 0.28 μM.

Table 1: Summary of Dissociation Constants for Cofactor Analogues

cofactor	K_d (μM)	$\Delta\Delta G_b$ (kcal/mol)
AdoCbl	0.17 ± 0.012	
AdoCbi	0.62 ± 0.09	−0.69
AdoCbi-PMe	3.33 ± 0.028	−1.64

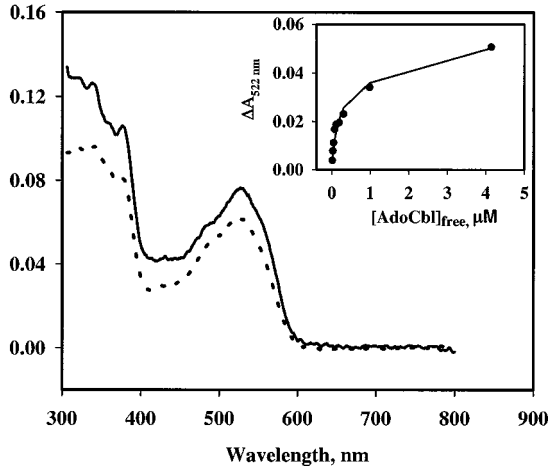

FIGURE 4: UV−visible spectra of free and enzyme-bound AdoCbl. The dotted line represents the spectrum of 7.4 μM free AdoCbl, and the solid line is the spectrum of 7.4 μM AdoCbl with 19.6 μM methylmalonyl-CoA mutase. Inset: Plot of ΔA_{522} as a function of free AdoCbl concentration at equilibrium. The concentration of free AdoCbl was calculated using eqs 2 and 3 using a value of K_d for AdoCbl of 0.17 μM (as described in Figure 3A legend). The solid line represents a fit obtained with eq 4.

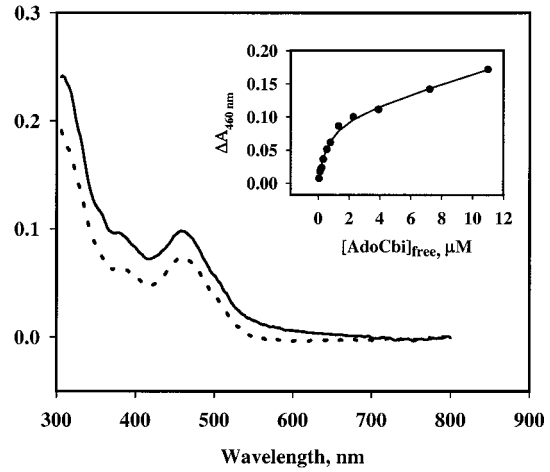

FIGURE 5: UV−visible spectra of free and enzyme-bound AdoCbi. The dotted line represents the spectrum of 8.6 μM free AdoCbi, and the solid line is the spectrum of 8.6 μM AdoCbi with 32 μM methylmalonyl-CoA mutase. Inset: Plot of ΔA_{460} as a function of free AdoCbi at equilibrium. $[AdoCbi]_{free}$ was calculated at each point using eqs 2 and 3 using a value of K_d for AdoCbi of 0.62 μM (as described in Figure 3B legend). The solid line represents a fit obtained with eq 4.

of methylmalonyl-CoA mutase, which binds B_{12}, has 11 tryptophan residues. While the residues that report on the conformational change accompanying cofactor binding are unknown, it is interesting to note that W334 is fairly close to the cofactor and may experience the most significant change in its environment following cofactor binding. The fluorescence change accompanying cofactor binding was employed to determine the equilibrium binding constants for

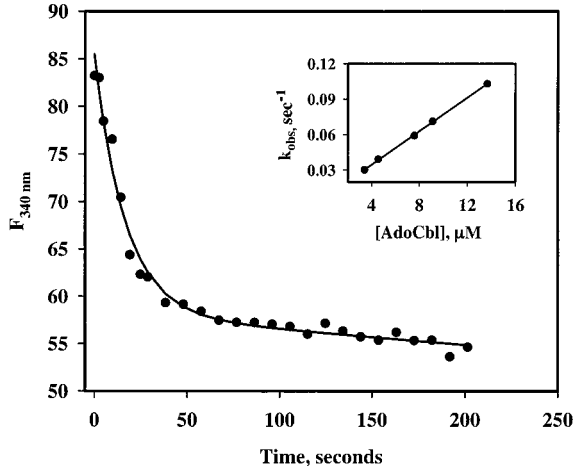

FIGURE 6: Kinetic analysis of AdoCbl binding to methylmalonyl-CoA mutase. Concentrations of AdoCbl and methylmalonyl-CoA mutase after mixing were 7.6 and 0.4 μM, respectively. Data were fit to eq 5 and yielded an observed rate constant, k_{obs}, of 5.9×10^{-2} s^{-1}. Inset: dependence of k_{obs} on AdoCbl concentration (from 3.4 to 13.7 μM). The slope of the best fit line gives k_{on} at pH 7.28.

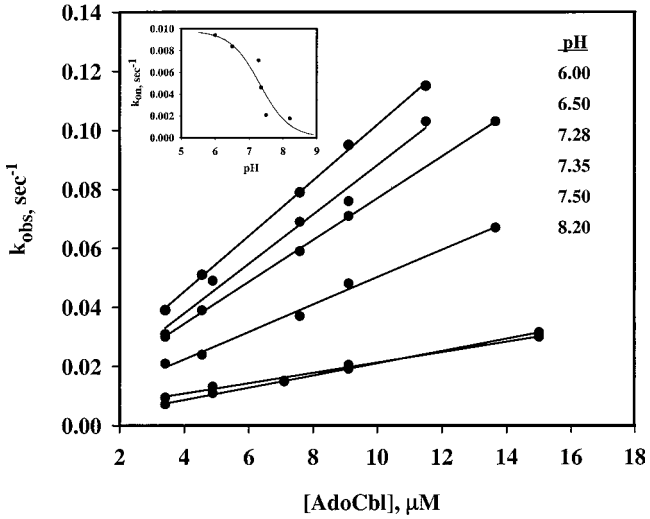

FIGURE 7: Dependence of fluorescence decay rates on AdoCbl concentration at different pH values. Inset: Dependence of k_{on} for AdoCbl binding on pH. The k_{on} values determined in Figure 7 were plotted as a function of pH. A value of 7.32 ± 0.19 is obtained for the pK_a from this analysis.

all three cobalamin derivatives (Table 1), and to study the kinetics of association with AdoCbl under stopped-flow conditions (Figure 7).

Both AdoCbi and AdoCbi-PMe lack the appended dimethylbenzimidazole tail, and are, perforce, base-off. This is readily confirmed by their absorption maximum being at 460 nm rather than 525 nm observed for base-on AdoCbl at physiological pH (*30*). Remarkably, loss of the nucleotide tail has a modest effect on the binding of these cofactor analogues to methylmalonyl-CoA mutase. Hence, AdoCbi, missing the nucleotide moiety, has a 3.5-fold higher K_d than AdoCbl, which corresponds to a difference in the Gibbs free energy of only -0.7 kcal/mol (Table 1). Addition of the phosphate methylester to AdoCbi extends the tail but results in an ~20-fold weakening in the association between the cofactor and enzyme. This is contrary to what may have been expected a priori, i.e., an incremental recovery of some of the favorable binding energy by an incremental increase in the length of the nucleotide tail. However, the phosphate appears to be involved in electrostatic interactions with water molecules in the dimethylbenzimidazole binding pocket (*3*), and it is possible that the presence of the nucleoside is required to facilitate these. The conclusion from these studies is that the nucleotide tail contributes approximately 1 kcal/mol to the binding interactions between AdoCbl and methylmalonyl-CoA mutase, and that the relatively tight binding of AdoCbl must be due to multiple interactions between the protein and corrin side chains.

The persistence of the base-off conformation of AdoCbi (Figure 5) and AdoCbi-PMe (not shown) in the mutase active site is surprising given the existence of His610 in the vicinity. This suggests that the absence of the nucleoside results in failure of the cofactor to organize the disordered loop into a rigid α-helix that steers His610 into the coordination sphere of the cobalt.[2] This is accompanied by the inability of the truncated cofactor analogues to support catalytic activity. This is most likely due to the interactions between the IIα2 helix in methylmalonyl-CoA mutase and the N-terminal domain of the α-subunit that are likely to be important in organization of the active site. Since mutation of His610 to alanine results in significant retention of enzyme activity (Chakraborty and Banerjee, unpublished results), the lack of coordination by this residue could not be the explanation for the failure of AdoCbi and AdoCbi-PMe to support enzymatic activity. In combination with the binding data presented above, these observations lead to the conclusion that the intrinsic cofactor binding energy is primarily utilized to reorganize the enzyme active site, and that these distal effects are essential for catalysis.

Binding of AdoCbl to the enzyme is accompanied by electronic changes in the spectrum (Figure 4). Notably, the shoulder at 377 nm is more pronounced in the spectrum of the bound cofactor, and there is a general increase in absorption across the 310−560 nm range. This is similar to the spectra reported for OHCbl in which an increase in the molar absorptivities was reported for the α, β, and γ bands on decreasing the polarity of the solvent (*31*). Hence, the spectral changes associated with AdoCbl binding to methylmalonyl-CoA mutase suggest sequestration in an active site with a lower dielectric constant relative to water.

The kinetics of AdoCbl binding to the mutase were studied by stopped-flow fluorescence spectroscopy. In solution, the equilibrium between the base-on and base-off species of

[2] We have previously reported that binding of AdoCbi to methylmalonyl-CoA mutase is accompanied by a red shift in the spectrum and interpreted this as evidence for histidine coordination to AdoCbi in the active site (*2*). This conclusion was, however, in error, since a closer examination of the published spectrum reveals it to be that of hydroxocobinamide (characterized by a prominent absorption maximum at 350 nm). In that experiment, enzyme treated with AdoCbi was purified by gel filtration chromatography in the dark to separate unbound cofactor. We have since repeated this experiment 3 times and each time have noted loss of the adenosine moiety and formation of hydroxocobinamide, although under identical conditions used routinely in the laboratory, the enzyme retains the adenosine moiety of AdoCbl! The difference in the lability of the two cofactor forms bound to the mutase is similar to the higher rate of photolysis of base-off methylcobalamin in the His759G mutant of methionine synthase (*34*) as well as to similar observations made with model compounds (*35*). During the time course of the binding titrations reported in this study, homolysis of AdoCbi and AdoCbi-PMe was not a problem. We thank Dr. John Pratt for pointing out the error in the spectral assignment in Figure 1 (*2*).

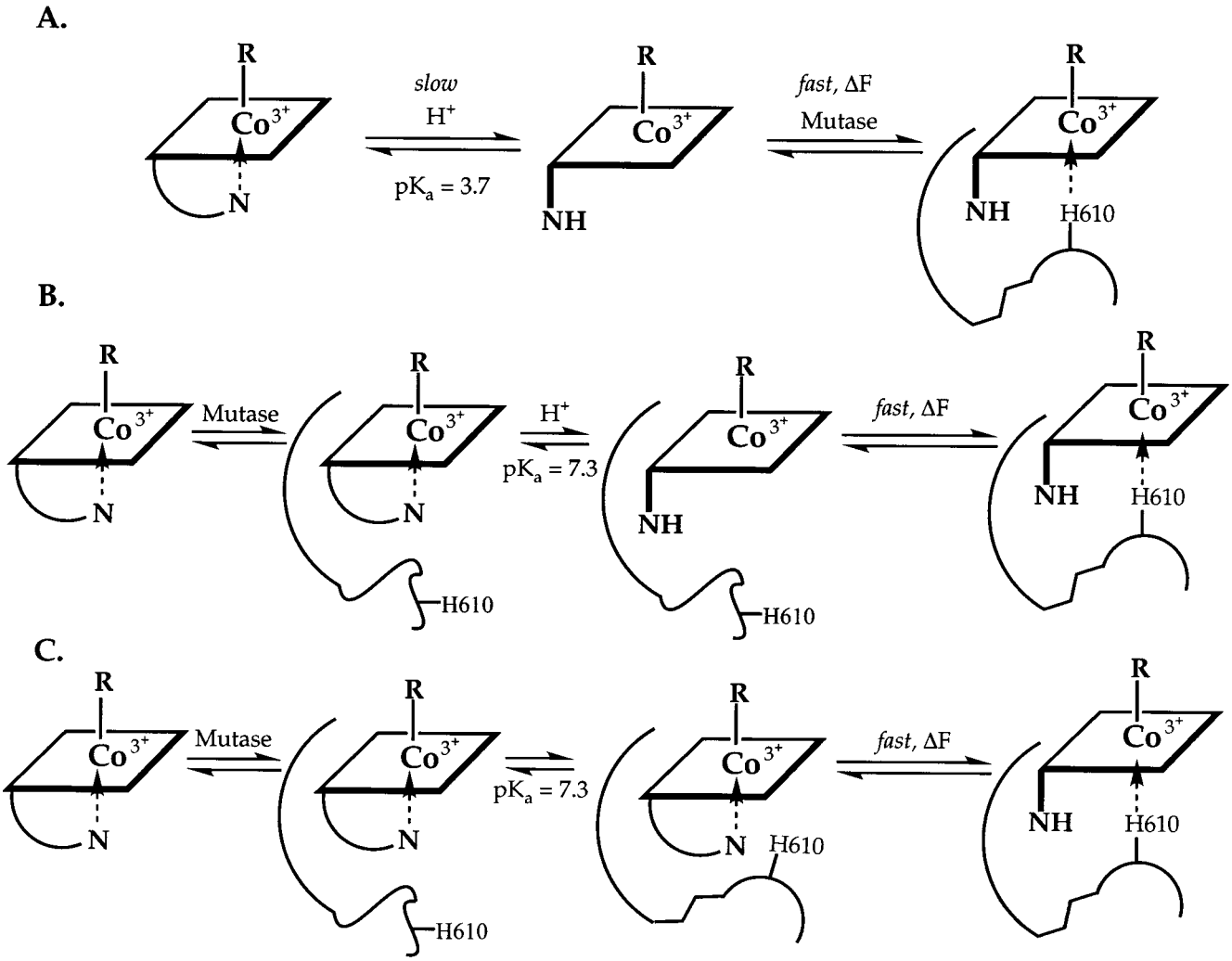

FIGURE 8: Alternative mechanisms describing binding of AdoCbl to methylmalonyl-CoA mutase. The difference between the upper and lower two pathways is that protonation of dimethylbenzimidazole occurs in solution in pathway A and in an enzyme−cofactor complex in pathway B. In pathway B, the pH-sensitive step is ascribed to a protein-linked pK_a for deprotonation of dimethylbenzimidazole whereas in pathway C it is ascribed to a conformational change in the protein. Δ*F* refers to the fluorescently sensitive step.

AdoCbl is governed by the pK_a of the dimethylbenzimidazole base, which is 3.7 (*32*). In the simple model described in Figure 8A, protonation of the cofactor in solution leads to the base-off state, which then rapidly associates with the enzyme in a step that results in fluorescence changes. At physiological pH, the slow step in this mechanism would be protonation of the base since the equilibrium would greatly favor the base-on species. If this mechanism accurately described binding of AdoCbl to methylmalonyl-CoA mutase, then the k_{on} would increase with decreasing pH, titrating to a pK_a of 3.7. Instead, the pH dependence of k_{on} for AdoCbl titrates to a pK_a of 7.3 ± 0.19, suggesting an enzyme-assisted deprotonation of the cofactor in the active site (Figure 8B, C). According to the model in Figure 8B, the slow step precedes formation of the base-off species. However, this conformational change occurs in a preassociation complex, accounting for the observed perturbation of the pK_a toward physiological pH. This is followed by rapid docking of the base-off cofactor in the active site, in a fluorescently sensitive step. Alternatively, the pH-sensitive step could represent a conformational change in the protein rather than the cofactor that precedes ligand substitution by His610 in the active site (Figure 8C). In both models, the fluorescently sensitive step must follow the pH-sensitive step. If the preassociation step resulted in fluorescence changes, then it would be difficult to explain why the kinetics of AdoCbi and AdoCbi-PMe association are too rapid to be measured but those of AdoCbl are not. The slow association of AdoCbl with methylmalonyl-CoA mutase is consistent with the >30-fold faster homolysis of the cobalt−carbon bond under turnover conditions when holoenzyme is mixed with substrate versus when apoenzyme is mixed with substrate and cofactor (*33*).

In summary, these studies provide the first evaluation of the relative importance of the nucleotide loop in AdoCbl to binding versus catalysis in a B_{12}-dependent enzyme that binds the cofactor in a base-off, "histidine-on" conformation. The cofactor binding energy contributed by the nucleotide tail appears to play a critical role in the organization of the active site and in steering the histidine residue into the correct orientation for ligation to cobalt. In contrast, the nucleotide tail makes a minor contribution to the affinity of the cofactor for the enzyme. The slow step in the binding of the cofactor involves the conformational change to the base-off state that is assisted by the enzyme, and is bypassed in analogues lacking the base.

ACKNOWLEDGMENT

We gratefully acknowledge Dr. Lawrence Schopfer (Eppley Institute, University of Nebraska Medical Center) for his help with the kinetic analysis of AdoCbl binding.

REFERENCES

1. Marsh, E. N. G., and Holloway, D. E. (1992) *FEBS Lett. 310*, 167−170.
2. Padmakumar, R., Taoka, S., Padmakumar, R., and Banerjee, R. (1995) *J. Am. Chem. Soc. 117*, 7033−7034.
3. Mancia, F., Keep, N. H., Nakagawa, A., Leadlay, P. F., McSweeney, S., Rasmussen, B., Bösecke, P., Diat, O., and Evans, P. R. (1996) *Structure 4*, 339−350.
4. Zelder, O., Beatrix, B., Kroll, F., and Buckel, W. (1995) *FEBS Lett. 369*, 252−254.
5. Drennan, C. L., Huang, S., Drummond, J. T., Matthews, R., and Ludwig, M. L. (1994) *Science 266*, 1669−1674.
6. Harms, U., and Thauer, R. K. (1996) *Eur. J. Biochem. 241*, 149−154.
7. Yamanishi, M., Yamada, S., Muguruma, H., Murakami, Y., Tobimatsu, T., Ishida, A., Yamauchi, J., and Toraya, T. (1998) *Biochemistry 37*, 4799−4803.
8. Lawrence, C. C., Gerfen, G. J., Samano, V., Nitsche, R., Robins, M. J., Retey, J., and Stubbe, J., (1999) *J. Biol. Chem. 274*, 7039−7042.
9. Banerjee, R. (1997) *Chem. Biol. 4*, 175−186.
10. Ludwig, M. L., and Matthews, R. G. (1997) *Annu. Rev. Biochem. 66*, 269−313.
11. Grate, J. H., and Schrauzer, G. N. (1979) *J. Am. Chem. Soc. 101*, 4601−4611.
12. Marzilli, L. G., Toscano, J., Randaccio, L., Bresciani-Pahor, N., and Calligaris, M. (1979) *J. Am. Chem. Soc. 101*, 6754−6756.
13. Chemaly, S. M., and Pratt, J. M. (1980) *J. Chem. Soc., Dalton Trans.*, 2274−2281.
14. Krouwer, J. S., Holmquist, B., Kipnes, R. S., and Babior, B. M. (1980) *Biochim. Biophys. Acta 612*, 153−159.
15. Ng, F. T. T., and Rempel, G. L. (1982) *J. Am. Chem. Soc. 104*, 621−623.
16. Geno, M. K., and Halpern, J. (1987) *J. Am. Chem. Soc. 109*, 1238−1240.
17. Halpern, J., Kim, S.-H., and Leung, T. W. (1984) *J. Am. Chem. Soc. 106*, 8317−8319.
18. Bresciani-Pahor, N., Forcolin, M., Marzilli, L. G., Randaccio, L., Summers, M. F., and Toscano, P. J. (1985) *Coord. Chem. Rev. 63*, 1−125.
19. Brown, K. L., and Brooks, H. B. (1991) *Inorg. Chem. 30*, 3420−3430.
20. Mancia, F., and Evans, P. (1998) *Structure 6*, 711−720.
21. Tollinger, M., Konrat, R., Hilbert, B. H., Marsh, E. N. G., and Krauetler, B. (1998) *Structure 6*, 1021−1033.
22. McKie, N., Keep, N. H., Patchett, M. L., and Leadlay, P. F. (1990) *Biochem. J. 269*, 293−298.
23. Padmakumar, R., and Banerjee, R. (1995) *J. Biol. Chem. 270*, 9295−9300.
24. Taoka, S., Padmakumar, R., Lai, M., Liu, H., and Banerjee, R. (1994) *J. Biol. Chem. 269*, 31630−31634.
25. Ishida, A., and Toraya, T. (1993) *Biochemistry 32*, 1535−1540.
26. Stinson, R. A., and Holbrook, J. J. (1973) *Biochem. J. 131*, 719−728.
27. Calafat, A. M., Taoka, S., Puckett, J. M. J., Semerad, C., Yan, H., Luo, L., Chen, H., Banerjee, R., and Marzilli, L. G. (1995) *Biochemistry 34*, 14125−14130.
28. Macara, I. G., and Cantley, L. C. (1981) *Biochemistry 20*, 5095−5105.
29. Thomä, N. H., and Leadlay, P. F. (1996) *Protein Sci. 5*, 1922−1927.
30. Giannotti, C. (1982) in B_{12}, pp 394−430, John Wiley and Sons, New York.
31. Hill, J. A., Pratt, J. M., and Williams, R. J. P. (1964) *J. Chem. Soc.*, 5149−5153.
32. Brown, K. L., Hakimi, J. M., and Jacobsen, D. W. (1984) *J. Am. Chem. Soc. 106*, 7894−7899.
33. Padmakumar, R., Padmakumar, R., and Banerjee, R. (1997) *Biochemistry 36*, 3713−3718.
34. Jarrett, J. T., Amaratunga, M., Drennan, C. L., Scholten, J. D., Sands, R. H., Ludwig, M. L., and Matthews, R. G. (1996) *Biochemistry 35*, 2464−2475.
35. Ng, F. T. T., Rempel, G. L., and Halpern, J. (1982) *J. Am. Chem. Soc. 104*, 621−623.

BI9914762